3
Fabrication & Characterization of microhotplate for metal oxide gas sensors

In this chapter, we discussed a new rapid prototyping method for the fabrication of an Au microheater and interdigitated electrode (IDE), which is a crucial part of any metal oxide based gas sensor platform. First, co-plannar meander shaped microheater and interdigitated electrodes (IDE) were fabricated via laser ablation technique. Au microheater and IDE were realized by ablation of sputtered deposited Au thin film on alumina substrate. Heat distribution profile, Temperature Coefficient of Resistance (TCR), long-term reliability at self-heating mode of the developed microheater were systematically investigated. The surface morphology and geometrical changes of metal lines were observed by SEM. In the last part of this chapter, we also observed the heat distribution profile and working temperature versus applied DC bias voltage of a commercially available hollow alumina tube based gas sensor platform through which a nichrome (Ni-Cr) heater coil was inserted.

3.1 Introduction

Mostly metal oxide semiconductors based chemiresistive type gas sensors are used for the detection of formaldehyde gases, for their low-cost, high potential of miniaturization, real-time detection of gases and ease to integrate with the system, minimum circuit requirement [Joshi et al., 2018; Liu et al., 2012; Wetchakun et al., 2011]. The gas sensing performance of metal oxide material has been observed at elevated temperature and for that purpose, a microheater based microhotplate is attached to the gas sensing layer to supply the heat to the sensing layer.

The last few decades, many metals and nonmetals such as platinum[Bíró et al., 2017], gold[Chau et al., 2012], polysilicon[Puigcorbe, n.d.], molybdenum[Mele et al., 2012], nichrome [Semancik et al., 2001], and tungsten [Syed Z. Ali, 2008] are using as a microheater material for the development of metal oxide gas sensors platform, and they are fabricating using conventional CMOS photolithography based microfabrication methods. Moreover, in this fabrication method, there is a requirement of health hazardous chemicals, costly and sophisticated equipment, a huge area of precisely maintained cleanroom facility, and lengthy process time. So, researchers are putting lots of effort into finding a user friendly simple, cost effective and rapid prototyping methods for the development of metal oxide sensors to overcome traditional photolithographic-based techniques.

In recent, the fabrication of sensor devices using laser micromachining technique via laser beam scanning is shown to be an efficient and cost-effective method for rapid prototype buildup and development of micro heaters or other types of microsensors on alumina and other flexible substrates [Chen et al., 2004; Liu et al., 1997; Rizvi, 2003]. Direct-write laser patterning technique shows great potential for the rapid prototype development of microheater of a gas sensor platform. In our thesis work, we have developed gold (Au) microheater based gas sensor platform with Au interdigitated electrode (IDE) to deposit a gas sensing layer on it. Here, Au has been used as a microheater due to some inherent properties such as high thermal conductivity (317 W/m-K), high working temperature (up to 1064°C) and it has high measurable positive linear temperature coefficient of resistance (TCR) (3.4×10^{-3}/°C) in the temperature range of 800°C [Chau et al., 2012]. Moreover, Au fulfilled both the requirements: microheater and metal electrodes and we get this by a single metallization process of gold. In addition, there is a requirement for an extra Au metal layer in the contact pad area of any sensor during wire bonding and we have observed this for the platinum and other heater materials, [Xie et al., 2010a]. On the other hand, if we use Au as a microheater and electrode, no extra metallization process is required in the pad areas for wire bonding during packaging. So, fabrication process cost can be reduced by using single metallization process. Furthermore, the

enhanced gas sensing behavior can be observed by the catalytic behaviour of Au from this approach [Li et al., 2011a].

3.2 Experimental details

3.2.1 Fabrication of Au Microheater and Interdigitated Electrode (IDE)

The co-plannar configuration of the microheater and IDE pattern were fabricated on a 500 μm-thick alumina (Al_2O_3) substrate of size 25.4 mm × 25.4 mm. Before fabrication, a coplanar configuration of microheater and IDE pattern layout was designed, as shown in figure 3.1 (a). The proposed fabrication process flow of the gas sensor platform is shown in figure 3.1 (a) – (c) and the schematic of the platform is shown in figure 3.1 (b). After proper cleaning of the alumina substrate (Figure 3.2 (b)), the substrates were placed in the sputtering chamber to deposit the Ti/Au metal layer. The thickness of Ti seed layer and Au metal layer were 20 nm and 200 nm, respectively. For the metalization, we have used DC sputtering (TFSP-840, VST Israel) technique (Figure 3.2 (b)). For this purpose, 3″ pure gold (Au) and titanium (Ti) targets were used. During deposition, the applied DC power to the Au and Ti target was 300 and 200 W, respectively. After deposition of the Ti/Au metallic layer on the IDE, the samples were annealed in order to stabilize their microstructure in nitrogen ambient for 5 hours at 300°C. The schematic of the laser ablation system is shown in figure 3.2. For patterning of Ti/Au thin layer, a Q-switched (Pulse repetition frequency = 30 KHz) solid-state ($Nd:YVO_4$) nano-second (pulse width of 20 ns) laser of 355 nm wavelength (Photonics Industries International Inc, USA) was used (Figure 3.2). A co-plannar configuration of microheater and interdigitated electrodes (IDE) were patterned on the substrate by ablation of Ti/Au metallic thin film layer by scanning with a focused laser beam having a spot size of 20 μm diameter and 0.75 W laser power, as shown in figure 3.2 (c). A gap of 400 μm was maintained between the microheater and electrode for electrical isolation, as shown in figure 3.1(b). The chips in the substrate were separated via laser scribing for packaging and bonding. The separated chips were mounted on a 4-pins ceramic package for wire bonding (Figure 3.3 (f)) to facilitate the electrical characterization. The final packaged gas sensor platform with microheater and electrode is shown in figure 3.3 (g).

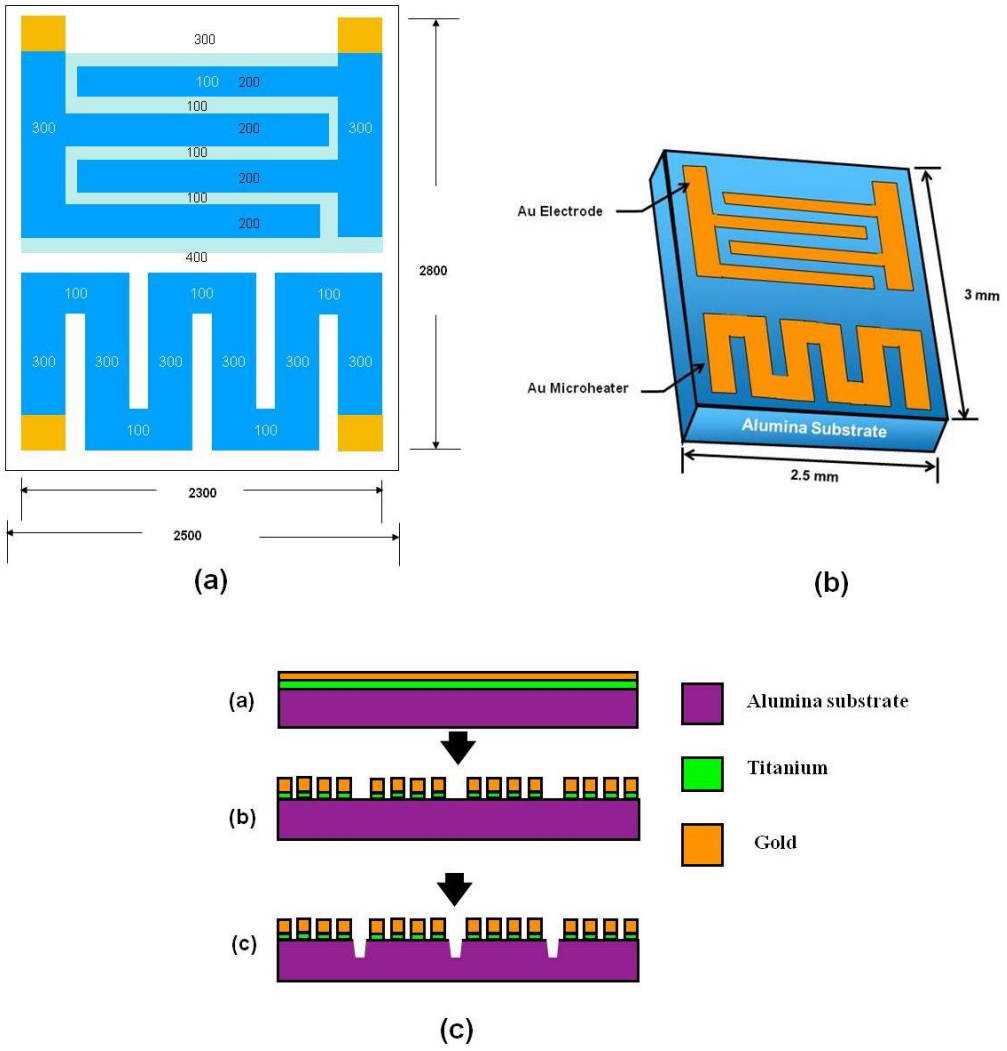

Figure 3.1: (a) Layout of the gas sensor platform with microheater and interdigitated electrode (IDE), all the dimensions in micron. (b) Schematic diagram of proposed gas sensor platform. (c) Process flow diagram for the fabrication of gas sensor platform.

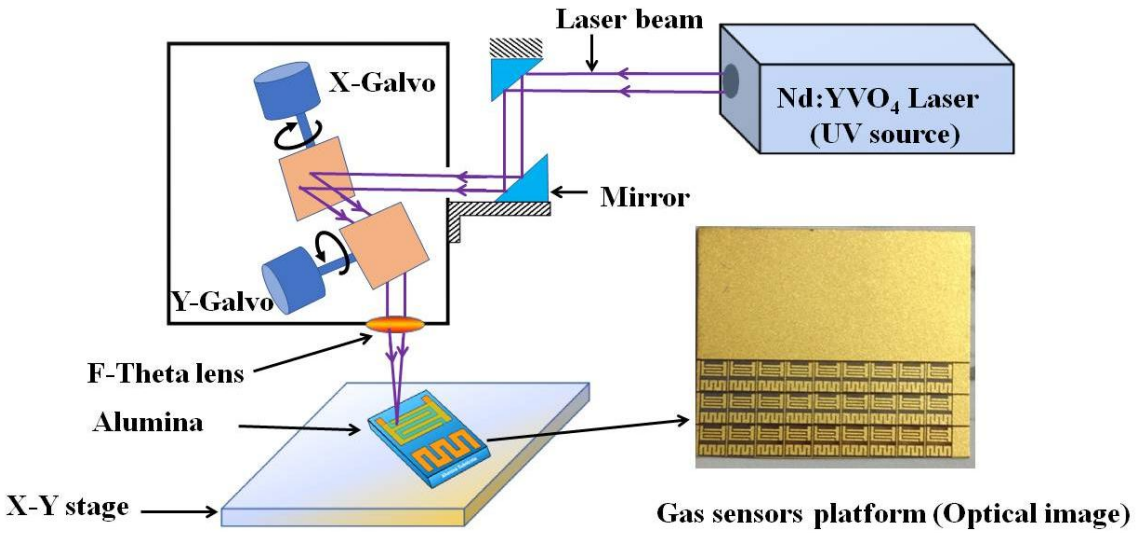

Figure 3.2: Schematic diagram of Pulse Laser Ablation (PLA) system.

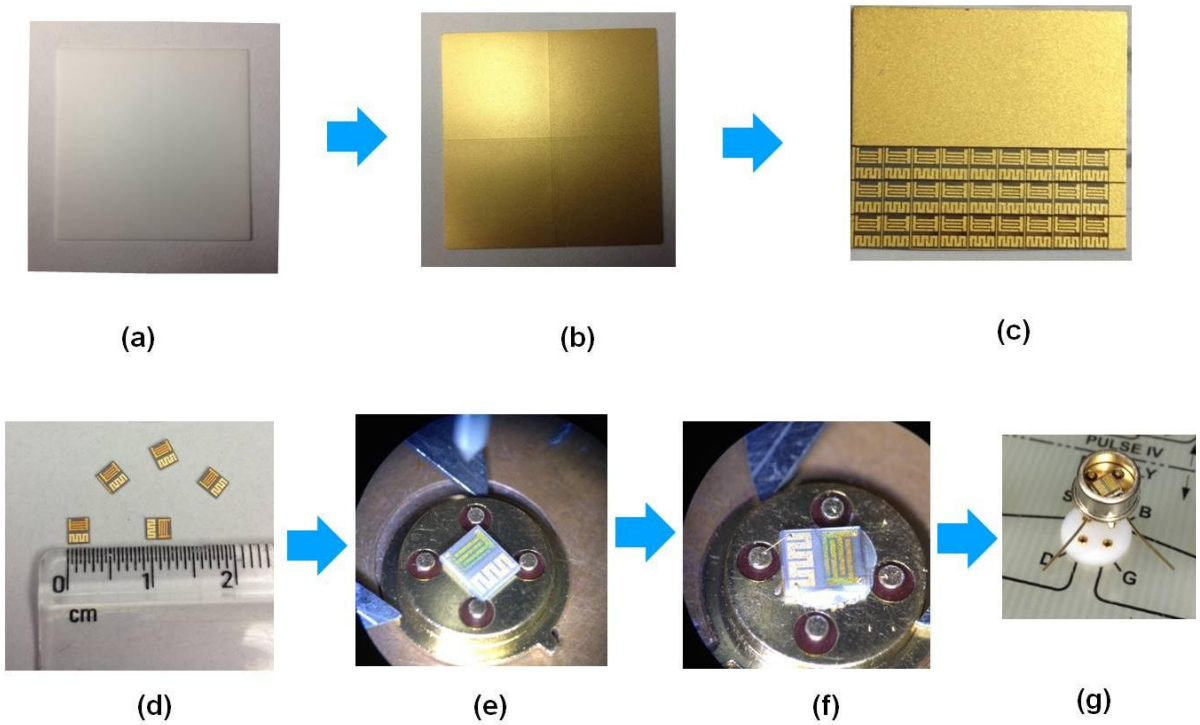

Figure 3.3: (a) Clean alumina substrate. (b) Sputtered deposited Ti/Au thin film on alumina substrate. (c) Realization of microheater and IDE pattern after laser ablation. (d) Diced chip. (e) Packaged chip on TO-39 header. (f) Wire-bonded chip for electrical characterization. (g) Packaged gas sensor platform.

3.2.2 Characterization of Au microheater based gas sensor platform

The geometrical structures of laser-ablated metal lines of the fabricated microheater devices were observed by scanning electron microscopy (FESEM, FEI Apreo). The thickness of sputtered deposited Ti/Au metal thin-film was measured by a stylus profiler (DektakXT® Bruker) based system. The sheet resistance of the sputtered deposited Ti/Au metal thin-film was measured by the 4-point probe (VEECO FPP-5000). We have also investigated systematically various parameters of the microheater, such as short- and long-term reliability, Temperature Coefficient of Resistance (TCR), and heat distribution gradient of the fabricated Au microheater based microhotplate.

3.3 Results and Discussions

3.3.1 Structural characterization of microheater

After the development of Au microheater and interdigitated electrode (IDE) via laser ablation process, the physical dimensions of the fabricated metal lines of the microheater and interdigitated electrode (IDE) were measured from the obtained scanning electron microscope (SEM) images (Figure 3.4 (a)). It was observed that the width of the fabricated metal line of the microheater and interdigitated electrode (IDE) has been reduced from its designed size of 300 µm to 245 µm (reduced 18%) and from 200 to 141 µm (reduced 29%), respectively as shown in figure 3.4 (b). It was also observed in the SEM images that the line-to-line spacing of the fabricated microheater and interdigitated electrode (IDE) are raised from the designed size of 100 µm to 125 µm (increased 25%) and from 100 to 110 µm (increased 10%), respectively. The change in dimension of the fabricated metal lines of the microheater and interdigitated electrode (IDE) has been observed due to the ablation of the metal line by the scattering of the laser beam from its focus point to the edge region of the metal line.

3.3.2 Measurement of resistance of the fabricated microheater

After physical vapor deposition (PVD) of Ti/Au metal thin films on an alumina substrate, the sheet resistance of the as-deposited Ti/Au metal thin films was about 0.201 Ω /

sq., and from the measured value, the resistivity of as-deposited Ti/Au thin films was calculated by

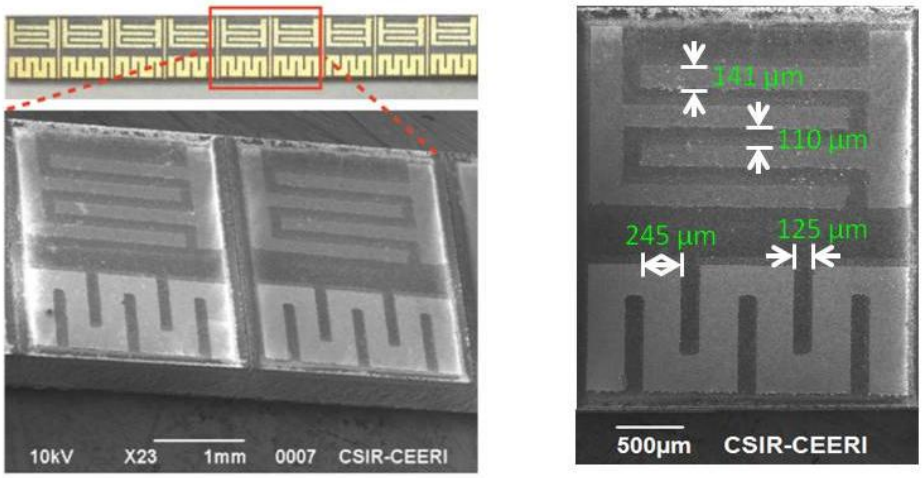

Figure 3.4: (a) FESEM images of fabricated Au microheater and IDE on alumina substrate. (b) High magnification FESEM images of microhotplate.

multiplying the obtained sheet resistance with the measured thickness (200 nm) of the thin film, which was about 2.81×10^{-8} Ω-m. In addition, the resistance of the laser-patterned fabricated microheater was theoretically calculated using the standard following relation:

$$R= (\rho.L)/(W.t). \qquad (3.1)$$

where ρ is the electrical resistivity (2.81×10^{-8} Ω-m) of the Au thin film, L is the length (6500 µm) and W is the actual line width (245 µm) and t is the measured thickness (220 nm) of the microheater and it was found to be 3.13 Ω. The calculated value of resistance was cross-checked by measuring the resistance value of the fabricated microheater with a multimeter and the average measured resistance value was about 3.68 Ω. There was not too much difference between the calculated and measured value. Measurement of resistance was carried out randomly on three different devices. A standard deviation of about 0.053 Ω was observed during measurement. It indicates that the devices were too much uniform with higher yield obtained by the laser patterning process compared than other patterning processes like photolithography, which suffers from over chemical etching. After annealing of the fabricated sensor devices at 300°C for several hours (minimum 5 hours), the average resistance value of the microheaters was increased from 3.68 to about 12.64 Ω due to the re-orientation of the polycrystalline structure of Ti/Au thin metal on Al_2O_3 substrate.

3.3.3 Measurement of TCR and Electro-thermal analysis

In order to measure the temperature coefficient of resistance (TCR), the packaged device was kept on a temperature-controlled thermal chuck. To measure the TCR, the microheater needs to heat externally. Then temperature of the chuck was raised from room temperature, T_0 (25°C) to 300°C and decreased from 300°C to room temperature (25°C) in the steps of 25°C. During the heating and cooling of the chuck, the resistance of the microheater was measured instantaneously using a multimeter (Keithley 2001). The value of TCR (α) of microheater material was extracted from the equation 3.2[Rao et al., 2017]:

$$\alpha = [(R_T - R_0)/(R_0.\Delta T)] \qquad (3.2)$$

Where, R_0 is the resistance of the microheater material at room temperature T_0, R_T is the resistance of the microheater material at temperature T (here, 300°C) and $\Delta T = (T-T_0)$, is the difference between final and room temperature during measurements. It is clearly observed in figure 3.5 (a) that the change in resistance of the microheater material was linear throughout the entire heating and cooling cycle test range from room temperature up to 300°C without any hysteresis in their test value. The measurement procedure of TCR value was repeated over five heating and cooling cycles on a single device. During the experiment, enough time was

provided between two successive tests to ensure the temperature of the microheater which was attached to a thermal chuck, reached thermal equilibrium to get accurate test results. From the experimental test results, the value of the temperature coefficient of resistance (TCR) of Au microheater material was as 1.3×10^{-3}/°C, which is in good agreement with the reported test results in various research articles. It was observed that the experimental test results of the TCR value (1.3×10^{-3}/°C) of a sputtered deposited thin film of Au microheater material was less than the TCR of bulk gold metal (3.4×10^{-3}/°C). This mismatch of TCR value between a thin film of Au microheater material and bulk gold metal was obtained due to the porosity of the sputtered deposited metal thin film, metal to metal interface at the grain boundary of the titanium oxide underneath of the Au layer on Al_2O_3 substrate. But, the measured value of TCR of Au thin film of microheater material was still relevant for the development a system for temperature sensing.

In any microheater, it is also required to study the heater temperature and reliability in self-heating mode where the microheater will be heated by an external current source as proposed by Joule heating effect model. To study these effects, the temperature of the microheater was increased from room temperature (25°C) to 300°C by passing DC current from a variable dc power source across the microheater and during heating of microheater, the corresponding current value was recorded for further calculation which was drawn by the microheater. The temperature of the microhotplate was increased due to the flow of current through the gold metal line of microheater via the Joule heating effect. The change in temperature (T) of the microhotplate was easily calculated from the following equation (3.3):

$$T = [\{(R_T - R_0.)/(\alpha.R_0)\} + T_0] \qquad (3.3)$$

Where, R_T is the measured resistance at temperature T, R_0 is the initial resistance at room temperature (T_0), alpha (α) is the obtained TCR value of the microheater material from the previous experiment and T is the change in temperature of the microheater. In addition, the resistive dissipation power of the microheater material was calculated by multiplying the current with the voltage drop across the microheater. The change in temperature of the microheater as a function of applied DC electrical power is shown in figure 3.5 (b). It is observed that the change in temperature of the microhotplate was increased linearly with applied DC power. From the measurement data, it was observed that the microheater consumed 1.4 W dc power to change the microheater temperature up to 300°C from the room temperature with loss of heat in the surrounding atmosphere. It was monitored that the power consumption of the microheater was high compared with other micro-electro mechanical sensor (MEMS) because the sensor chip was thermally connected to ceramic package by epoxy which was acting as a heat sink for the microheater due to their direct contact with the substrate. Our aim was to fabricate a rapid prototype gas sensor platform with Au microheater and electrode and our microheater design was not truly optimized particularly for low power gas sensing applications. Various methods can be applied to reduce the power consumption of the microheater and one of the methods is the isolation of the chip from the metal TO-39 header.

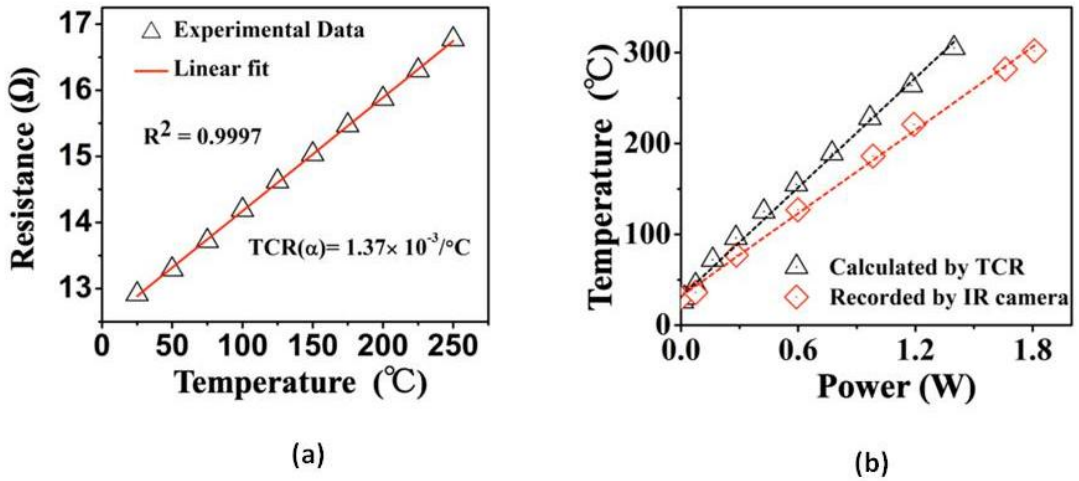

Figure 3.5 : (a) TCR of gold microheater and (b) Microheater temperature variation as a function of input power.

3.3.4 Measurement of Heat Distribution Profile of microhotplate

The heat distribution profile of the Au microhotplate was observed by keeping the fabricated sensor platform under a high-resolution infrared (IR) thermal camera (Figure 3.6 (a)). To observe the heat distribution profile with the temperature gradient of the microhotplate and obtain the microhotplate temperature, various value of DC current was applied across the two terminals of the microheater. Due to flow of current, the heat was produced in the sensor platform and the various current value was recorded as a function of applied voltage. Figure 3.6 (a) shows the heat distribution profile with temperature gradient of the Au microheater based gas sensor platform at 300°C operating temperature, where applied bias voltage across the microheater was 5.4 V. From figure 3.6 (b), we have observed that there is a negligible heat gradient and uniformity in temperature on the entire gas sensor platform. There is no difference in heat gradient observed between the active area of the microheater side and the IDE pattern of the gas sensor platform due to the high thermal conductivity of the alumina substrate. It is also seen in figure 3.6 (b) that the produced heat spreads very quickly from the gold microheater metal line to the alumina (Al_2O_3) substrate which was used as a platform material. In this context, we should mention that it was very difficult to detect the accurate temperature of the gold line on the alumina substrate due to the low emissivity of gold.

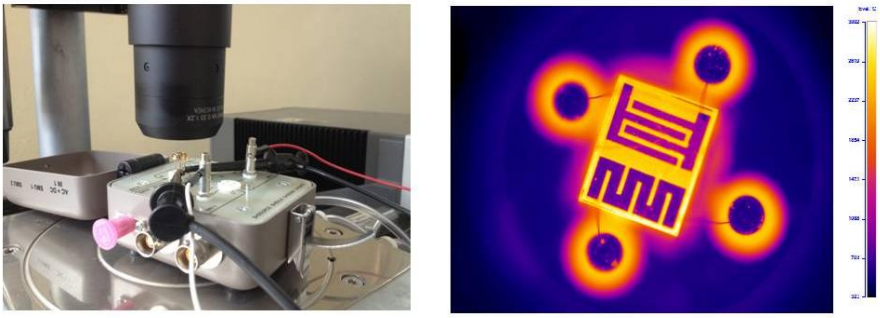

(a) (b)

Figure 3.6: (a) Microheater platform under IR based thermal imaging camera and (b) Heat distribution profile of the Au microheater based gas sensor platform.

3.3.5 Repeatability and Reliability test of microheater

Metal oxide gas sensors need to run long times (years) and it require frequent heating and cooling cycles during its operation. So, it is necessary to study the short-term repeatability behaviour of the microheater for various thermal cycles (heating and cooling). To study the short-term repeatability test, the microheater was heated up to 300°C temperature in ambient air for ten successive cycles in a regular time interval of 15 minutes via applying a DC bias voltage of 5.4 V. During heating and cooling cycles, the resistance of the microheater was recorded during heating and cooling cycle using LabVIEW based computer system. From figure 3.7 (b), it was observed that the change of resistance of the microheater for every heating cycle was the same i.e. it produced a fixed temperature of ~ 300°C for each thermal cycle and did not degrade due to thermal stress.

Furthermore, for the detection of gases using metal oxide based, the operating temperature of the metal oxide sensing layer has to be maintained precisely using the microheaters continuously for a long time (years). So, to test this properties of the microheater, the long-term reliability test of our fabricated Au microheater was investigated in the Joule heating mode at different temperatures (250°C, 300°C and 350°C) by passing a constant current through the two terminals of the microheater continuously for long-time. Figure 3.7 (c) and (d) exhibit the long-term reliability test results during the operation of the microheater at different operating temperatures for a long time in self-heating mode. During the long-term reliability test, the microheater was biased with a DC voltage source having various current densities and the corresponding resistance was recorded in five minute intervals for a long-time (330 hours). Figure 3.7 (c) shows the change in the resistance value of the microheater with time. After applying 4.5 V (current density 5×10^9 A/m^2) bias voltage ~ 250°C temperature was obtained in the microheater and it was monitored that in spite of prolonged heating, the microheater run reliably at temperature 250°C for 330 hours with negligible drift in resistance value (< 0.5 %), as shown in figure 3.7 (c). But, when the microheater was biased with DC voltage of 6.1 V with current density of 5.9×10^9 A/m^2, the microheater showed rapid change in its resistance at an average operating temperature of 350°C, as shown in figure 3.7 (d). This rapid change in resistance was occurred due to the electromigration effect. Thus, in our proposed designed of microhotplate it was observed that the gold (Au) microheater was highly reliable up to 300°C without any oxidation of resistant, drift in resistance and electromigration. Furthermore, it was also observed that the gold (Au) microheater showed its excellent physical and electrical properties at 250°C temperature with high stability and repeatability. In addition, the metal line of Au microheater with 0.2 micron thickness sustained without any resistance drift at high current density of 5×10^9 A/m^2 at applied voltage of 4.5 V.

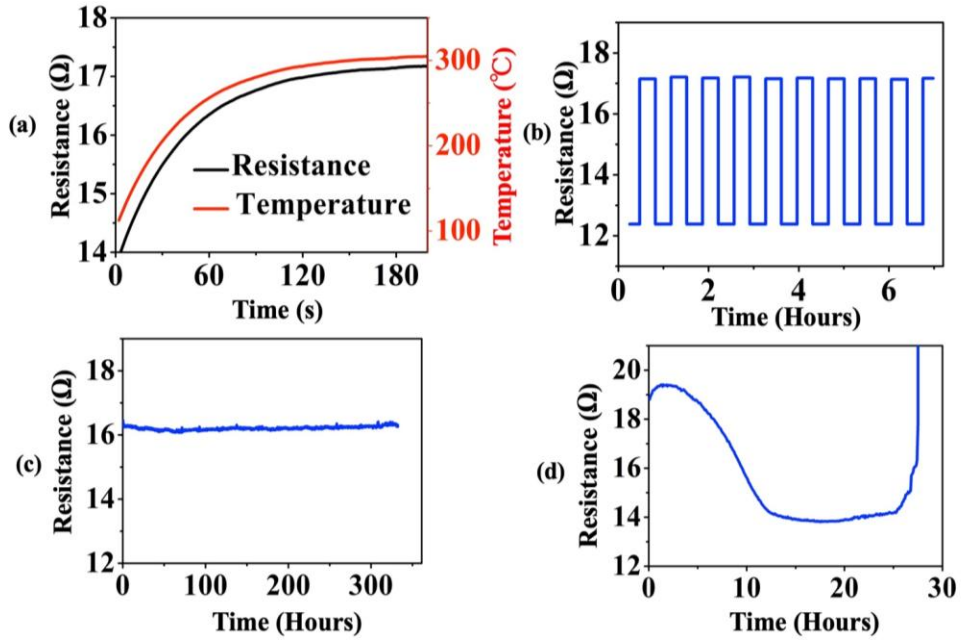

Figure 3.7: (a) Transient characteristic curve of the microhotplate at 300°C. (b) Changes in resistance of the microheater for ten successive thermal cycles at 300°C. (c) Changes in resistance of the microheater during long-term reliability test at 250°C. (d) Changes in resistance of the microheater during long-term reliability test at 350°C.

3.4 Characterization of Nichrome (Ni-Cr) heater based microhotplate

In the previous section, we have seen that the Au microheater based gas sensor platform can work up to 250°C and the gas sensor prototype can be built using a simple laser ablation process. But, we want to reduce the fabrication cost for making the gas sensor platform. So, we have used the commercially available gas sensor platform as an alternate source of low cost gas sensor platform. The gas sensor platform consisted of a hollow alumina tube, two Au electrodes at both ends of the tube and platinum wires connected with Au electrode for conducting the current through the sensing layer via Au electrode. The length, internal diameter and external diameter of hollow alumina tube gas sensor platform were 4 mm, 0.8 mm and 1.2 mm, respectively, as shown in figure 3.8 (a).These platinum wires were bonded onto the pins of the bakelite package and it helps to hang the platform for thermal isolation during operation. To produce the working temperature for the gas sensing layer, a nichrome coil was inserted through the hollow alumina tube and it maintains the operating temperature of the gas sensing layer in the range of 200 to 400°C. We have used a scanning electron microscope (SEM) to observe the actual structure of the gas sensor platform and the SEM image is shown in figure 3.8 (b). To know the operating temperature of the gas sensing material, it was required to characterize the microheater. And as a part of this test, the microheater was biased with a DC bias voltage source across the microheater, the heat was produced in the microheater by the Joule heating effect. The obtained temperature versus applied voltage was measured by an Infrared (IR) based thermal camera (AT-Automation Technology GmbH). Figure 3.9 (a) and figure 3.9 (b) exhibited the heat distribution profile and temperature versus applied d.c. bias voltage of the nichrome (Ni-Cr) heater based ceramic tube gas sensor platform, respectively. It was observed in figure 3.9 (a) that there was negligible heat gradient and better temperature uniformity on the gas sensor platform.

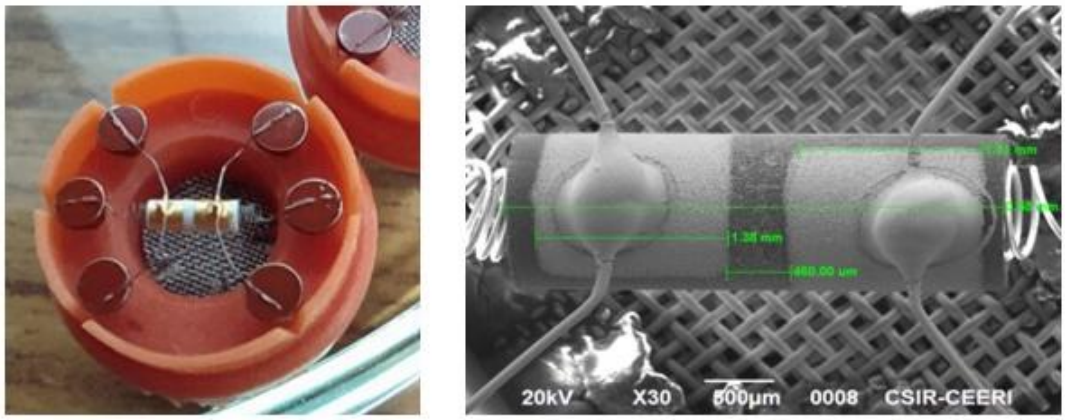

Figure 3.8: (a) Optical image of the Nichrome (Ni-Cr) heater based gas sensor platform. (b) SEM image of the electrode and Ni-Cr heater.

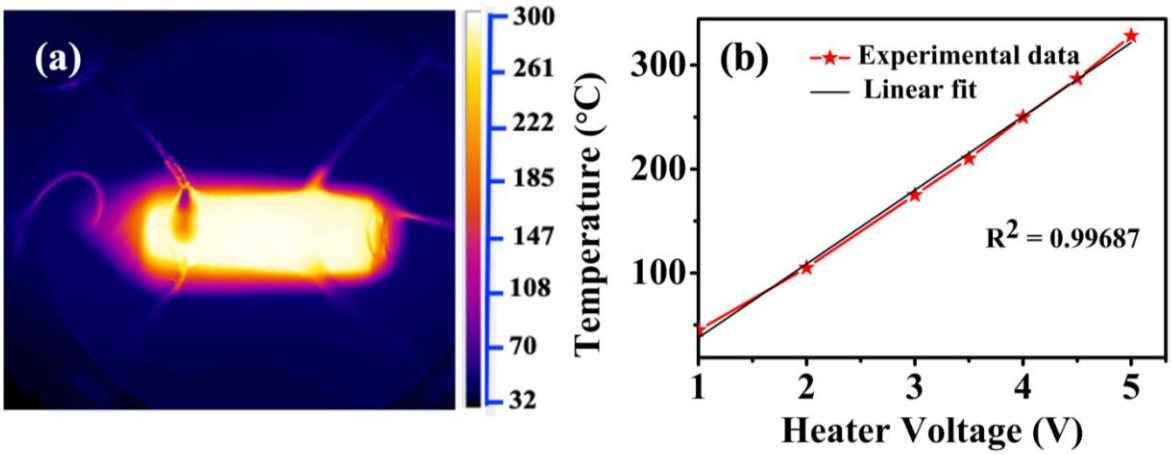

Figure 3.9: (a) Infrared thermal image of the ceramic tube gas sensor platform at 300°C. (b) Heater temperature versus applied d.c voltage across the Ni-Cr heater.

3.5 Conclusion

In this chapter, firstly, we have fabricated a rapid prototype of a gold microheater based gas sensor platform using a direct-write laser patterning method in air. The long-term reliability test of the Au microheater was carried out at an operating temperature of 250°C for 330 hours in self-heating mode and after heating long-time (330 hours), the Au microheater showed excellent stability and reliability with a nominal change in resistance value. However, the fabricated Au microheater based microhotplate platform with excellent uniformity in temperature distribution validated the potential of metal oxide-based gas sensors. Thus, the development of microhotplate by patterning of Au metal thin film using direct-laser ablation technique is a rapid prototype method which is a simple photo-maskless process for fabricating the microheater and IDE in a reproducible manner. The fabrication process cost and development time are also low and any hazardous chemicals are not used which is observed during resist based lithographic process. So, this laser ablation based microfabrication method has a huge potential to use as an alternative route instead of using the standard micro-lithography process for the batch production of the gas sensor platform. This study shows that an Au microheater can be a reliable and efficient gas sensors platform. Since microheaters are an essential component of any metal oxide-based sensors, development of microheaters paves the way for further metal oxide-based sensor development. In the last of this chapter, we also investigated the heat distribution profile and temperature versus applied voltage of the commercial gas sensor platform. The commercial gas sensor platform is a good choice for the researchers to use as a gas sensor platform for metal oxide materials at an affordable price. Hence, our further effort will be in the direction of developing metal oxide-based formaldehyde sensor using a commercially available Nichrome (Ni-Cr) heater based gas sensor platform.